

Presented at the Air
Pollution Control
Association International
Specialty Conference
"Visibility Protection-
Research and Policy
Aspects," Grand Teton
National Park, Wyoming,
September 7-10, 1986.

COMPARISON OF ATMOSPHERIC EXTINCTION MEASUREMENTS
MADE BY A TRANSMISSOMETER, INTEGRATING
NEPHELOMETER, AND TELERADIOMETER WITH NATURAL AND
ARTIFICIAL BLACK TARGET

William C. Malm, Air Quality Division, National
Park Service, CIRA - Foothills Campus, Colorado
State University, Fort Collins, CO 80523

Gerald Persha, OPTEC, Inc., 199 Smith Road, Lowell, MI 49331

Roger Tree, Air Resource Specialists, Inc., 634 S. Mason, Fort Collins, CO
80524

Roger Stocker, Department of Atmospheric Science, Colorado State University,
Fort Collins, CO 80523

Ivar Tombach, AeroVironment, Inc., 825 Myrtle Avenue, Monrovia, CA 91016-
3424.

Hari Iyer, Department of Statistics, Colorado State University, Fort Collins,
CO 80523

One essential variable for describing how image forming information is transmitted through the atmosphere is the atmospheric extinction coefficient. However, the two instruments routinely used to make extinction measurements, the integrating nephelometer and contrast teleradiometer using natural targets, have shortcomings which only allow for approximations of the extinction coefficient. The integrating nephelometer measures only atmospheric scattering, may modify aerosols that pass through its sampling chamber, and best measures scattering from small articles. Teleradiometers are limited in their ability to measure extinction because of errors in estimation of the inherent contrast and nonuniform illumination of the sight path. Two alternative techniques for measuring atmospheric extinction are transmissometry and contrast teleradiometry using artificial black targets. This paper presents results of a field study where all four techniques were intercompared. Errors in deriving atmospheric extinction from teleradiometer measurements due to nonuniform lighting and uncertainty in inherent contrast are discussed for artificial and natural targets. The error in transmissometer measurements resulting from atmospheric turbulence is also presented. Comparisons of extinction derived from each of the above

measurements show that correlations during daytime hours between transmissometer, nephelometer and contrast of artificial target were near 0.80, while correlation of any of these measurements with extinction determined from the contrast of a natural target was near 0.40. The slope of the regression line between transmissometer extinction and artificial target extinction was near one, while the slope of either the transmissometer or artificial target extinction against nephelometer extinction was near 0.65.

Introduction

Measurement of the extinction coefficient is essential to understanding how atmospheric aerosols affect the visibility of scenic vistas. However, accurate measurement of extinction in clean atmospheres and under all meteorological conditions poses a formidable problem. To date, the two methods routinely employed for estimating extinction are integrating nephelometry and teleradiometry using natural targets^{1,2}. Both measurement techniques have serious shortcomings. The integrating nephelometer measures atmospheric scattering and not absorption, may modify particles that pass through its sampling chamber and properly measures scattering from only fine particles. Calculations of atmospheric extinction using teleradiometer measurements of natural target contrast, on the other hand, are sensitive to both scattering and absorption, and measure effects of particles of all sizes in the ambient aerosol. However, the extinction calculation from the contrast measurement is sensitive to variations in inherent contrast and nonuniform illumination conditions, neither of which can be readily accounted for in normal measurements.³

Two measurements which are less sensitive to meteorological conditions and do not modify atmospheric aerosol by passing it through sampling chambers are transmissometry and teleradiometric measurements of sky target contrast of artificial target with a reflectivity that is near zero ($C_0 = -0.1$).

This paper discusses results of a measurement program conducted near Meteor Crater, Arizona in which a transmissometer, teleradiometer measuring sky-target contrast of a nearly black artificial target, teleradiometer measurements of sky-target contrast of a natural tree covered target, and an integrating nephelometer were used to measure atmospheric optical parameters from which, through the use of appropriate models, atmospheric extinction can be extracted.

Instrumentation

Table 1 summarizes teleradiometer characteristics as well as parameters, such as path lengths, associated with their physical layout. The teleradiometer used for natural target contrast measurements was a standard MRI 3010 Vista Ranger,⁴ while the teleradiometer used for the artificial black target, referred to as a precision teleradiometer, was a specially designed low flare small angle of view instrument built by Optec, Inc.⁵

The flare characteristics of the precision teleradiometer were experimentally measured using a small artificial black target designed such that it subtended the same angle at 12 m distance as did the larger artificial target at 3.3km. The teleradiometry flare was approximately 1% of the background radiance (radiance coming from behind the target) for all geometries considered. This was true whether the sight path sun angle geometry corresponded to forward or back scatter or whether the sky was cloudless or overcast.

The artificial target was a large 3m x 3m x 3m "box" with a 2.1m circular hole cut out of one side. The box was further "baffled" with three additional 7 ft circular apertures placed at 3ft intervals inside the box. Measurements of "box" radiance a few meters from the target using a standard 3010 teleradiometer⁶ showed target radiance to be below detection limits of the teleradiometer. For purposes of this study, C_0 was assumed to be identically equal to -0.1.

The transmissometer light source was designed using a 40 watt quartz halogen lamp calibrated to give a light output that is nearly constant over a 2° cone. The light source was modulated at 87.4 cycles/second. Transmissometer receiver optics were designed around a refracting F/5 630mm telescope fitted with a detector/operational amplifier combination similar to the 3010 teleradiometer.

The output of the amplifier was fed to a high Q (Q=30) band pass filter and to a zero-cross detector. The zero-cross detector was used to determine the precise time the light was turned from off to on. Establishing this "time line" is essential for determining when the signal should be sampled for purposes of calculating differences between teleradiometer signal when light source is off and when it is on. It is, of course, this difference signal that is proportional to the transmittance of the atmosphere. Radiance differences are measured 87 times per second and averaged for 1.5 minutes. This average value is presented as an analog signal between 0 and 300 millivolts.

Measurement Consideration

Teleradiometry Using Natural Targets

Teleradiometers measuring atmospheric radiance of sky and natural targets can be used in a number of ways to yield approximations of atmospheric extinction. However, the traditional method of making teleradiometric extinction measurements involves measuring sky and natural target radiance at some distance r and using:

$$C_r = C_0 \frac{s_{N_0}}{s_{N_r}} e^{-b_{ext} r} \quad 1)$$

to approximate b_{ext} ^{7,8}. C_r and C_0 are the apparent and inherent target contrasts respectively, s_{N_0} and s_{N_r} are the sky radiance at the target and observer, while r is the distance to the target and b_{ext} is the atmospheric extinction coefficient. Typically s_{N_0} and s_{N_r} are assumed to be equal and equation 1 is used to approximate C_0 when it is known that the atmosphere is near Rayleigh conditions, i.e., $b_{ext} \approx b_{ray}$. If it is assumed that $s_{N_0}/s_{N_r} \approx 1$, then equation 1 can be solved for b_{ext} ;

$$b_{ext} = -\frac{1}{r} \ln [C_r/C_0] \quad 2)$$

However, s_{N_0}/s_{N_r} is never exactly equal to one and, if the target isn't black, C_0 is dependent on lighting conditions, clouds behind the target and the atmospheric particulate loading (through a variation in s_{N_0} as a function of b_{ext}).

The error in calculated extinction associated with uncertainty in s_{N_0}/s_{N_r} and C_0 is

$$\frac{\delta b}{b} = -\frac{1}{b_{\text{ext}} r} \sqrt{\left[\frac{\delta \gamma}{\gamma}\right]^2 + \left[\frac{\delta C_0}{C_0}\right]^2} \quad 3)$$

where $\gamma = sN_0/sN_r$.

The variation of γ and C_0 for the teleradiometer target geometry used at Meteor Crater is examined as a function of atmospheric aerosol loading using a Monte Carlo radiation transfer calculation that explicitly accounts for earth curvature and higher order scattering.⁹ The target is 63km distant, and azimuth and observation "viewing" angles are 325° and +0.1° respectively. An azimuth viewing angle of 325° corresponds to a sun/sight path scattering angle of 158% (backscatter) at 9:00 a.m.

Figure 1 shows expected errors in calculated extinction for Rayleigh day inherent contrasts of -1.0, -0.8 and -0.6 as a function of aerosol extinction. The error in calculated extinction for $C_0 = -1.0$ is due only to changes in sN_0/sN_r as the aerosol loading is changed, while the error curves for $C_0 = -0.80$ and -0.60 show the additional error associated with variation in C_0 .

For a scattering angle of 158°, the sky becomes darker as b_{ext} increases and the absolute magnitude of the actual inherent contrast of any non-black target tends somewhat toward zero. Thus, as b_{ext} increases, there is an increasing error in C_0 and the error in "measured" extinction increases. The error is most pronounced for "back scatter" conditions and for targets with Rayleigh inherent contrasts smaller in magnitude than about 0.80. Figure 1 shows that for a Rayleigh C_0 of -0.60 the error in extinction exceeds 100% at $b_{\text{ext}} = 0.02 \text{ km}^{-1}$.

The previous discussion was for idealized conditions where the sky is free of clouds and illumination is uniform. Under meteorological conditions where clouds behind the target are either brighter or darker than the background sky, uncertainty in calculated extinction increases. More importantly, when clouds pass over the sight path, the path radiance is reduced. For optically thick summertime cumulus clouds, path radiance can be reduced by 70% or more.

Teleradiometry of Artificial Black Target

The above discussion applies to single teleradiometric measurements of sky target contrast of artificial targets as well as natural targets. However, when using an artificial target it is possible to construct a target that is nearly black. Examination of equation 3 and Figure 1 shows that when $C_0 = -0.1$ most of the error associated with calculating extinction from contrast measurements under standard illumination conditions is removed.

The only error associated with the extinction calculation is due to the uncertainty in sN_0/sN_r . For standard illumination conditions over the short path lengths ($r < 10 \text{ km}$) required for use of artificial black targets, $sN_0/sN_r \approx 1$ and little error is associated with determining extinction. Even under cloudy conditions where clouds behind the target are as much as 1.5 times brighter than background sky and are located at distances greater than 100 kilometers, radiation transfer calculations show that the error associated with calculating extinction from black box contrast is less than 15%. However, single teleradiometer contrast measurements of black targets are still subject to cloud shadows over the sight path ($sN_0 \approx sN_r$). Errors due to sight path shadowing can only be remedied by measuring sky radiance at the target (sN_0) and explicitly accounting for the ratio sN_0/sN_r .

Even though an artificial black target appears promising, a sensitivity analysis of path radiance as a function of target distance shows that the teleradiometers' accuracy and sensitivity must be extremely high. Differentiating equation 1 with respect to b_{ext} and assuming $sN_o = sN_r$ shows that the error in measured contrast relates to extinction error by

$$\frac{d C_r}{C_r} = -b_{\text{ext}} r \frac{d b_{\text{ext}}}{b_{\text{ext}}} \quad 4)$$

For a black target located 3.3 km distant from the teleradiometer, the path radiance on a Rayleigh day will be approximately 3.5% of the sky radiance. To measure Rayleigh extinction (0.01 km^{-1}) with an accuracy of near 10% would require a contrast measurement accuracy of less than 1/2%. Therefore, special care must be taken to carefully characterize teleradiometer flare characteristics.

Other considerations in using artificial black targets are the required target size and the problem of maintaining teleradiometer alignment on the black portion of the target. For instance, teleradiometer with 0.017° angle of view would require approximately a 1.0 m target at a path distance of 3.3 km. For purposes of maintaining alignment and reducing teleradiometer flare, the target was chosen to be twice as big or approximately 2.0 m in diameter.

When the teleradiometer is aligned so that it is centered on the black target, a shift in alignment of only 0.0085° moves the teleradiometer off target. Therefore, alignment was routinely checked to minimize drift in radiometer positioning.

Transmissometers

Historically, transmissometers have been thought of as teleradiometric measurements of the intensity of a light source placed at some distance r from an observation point.⁷ The equation governing the amount of radiant energy received at the observation point is

$$H = \frac{I_o}{r^2} e^{-b_{\text{ext}} r} \quad 5)$$

where H is irradiance at some distance r from the light source, I_o is radiant intensity and b_{ext} is the atmospheric extinction coefficient. I_o/r^2 is essentially a calibration term that can be determined by comparison of transmission measurements to other optical measurements such as teleradiometer measurements made under "standard" lighting conditions or to integrating nephelometer measurements made on days that are near the Rayleigh scattering limit. A second calibration technique and the one used in the measurement program utilizes measurement of a signal proportional to H at two different distances:

$$H_1 = \frac{I_o}{r_1^2} e^{-b_{\text{ext}} r_1} \quad 6)$$

$$H_2 = \frac{I_o}{r_2^2} e^{-b_{\text{ext}} r_2} \quad 7)$$

Measuring r_1 , r_2 , and a signal proportional to H_1 and H_2 , and assuming the atmosphere is homogeneous over distances r_1 and r_2 allows equations 6 and 7 to be solved for I_0 .¹⁰ For the Meteor Crater study, the two sight paths were 7.8 km and 3.05 km. If the measurement of H is carried out using a path that is open (versus a path that is enclosed within a sampling chamber) the calculated extinction will be independent of illumination conditions, will not be biased toward large or small particles and will include the effects of atmospheric absorption.

The sources of error in atmospheric transmission measurements are numerous. Middleton⁷ discusses errors in the early experiments that were due to light scattering from surfaces internal to optical instruments, nonlinearity of detection systems and stability of electronics. If path lengths are much beyond 2 km, atmospheric turbulence and beam refraction by atmospheric strata at different temperatures can degrade the transmitted light signal to a point where accurate determination of b_{ext} becomes difficult. Atmospheric turbulence is especially difficult to contend with when using lasers as the light source. The author has witnessed a laser beam transmission measurement over a path length of 10 km where at times a laser beam, focused to beam diameter of about 20 cm bloomed to over 10 meters in diameter as turbulence conditions changed.

In any case, whether the error is due to atmospheric turbulence or instrumentation design limitations, equation 5 can be differentiated with respect to $b_{ext} r$ to yield a relationship between error in measured optical depth ($b_{ext} r$) and error in the transmission measurement:

$$\frac{d(b_{ext} r)}{b_{ext} r} = \frac{1}{b_{ext} r} \frac{dT}{T} \quad 8)$$

Equation 8 shows the relationship between the percentage error in optical depth and percentage error in the measurement of transmittance. Figure 2 is a plot of error in optical depth $d(b_{ext} r)/b_{ext} r$ as a function of optical depth for values of $dT = 0.01$ and 0.02 . For path lengths of 1 km or less, T can typically be measured to 1% or less, i.e., $dT < 0.01$. On the other hand, for path lengths of about 10 km, atmospheric turbulence can limit the accuracy to about 2% ($dT \approx 0.02$). For the Meteor Crater experiment $r \approx 8$ km so on a Rayleigh day $b_{ext} r \approx 0.08$. Examination of Figure 2 shows that, depending on turbulence condition on a Rayleigh day, the measured atmospheric extinction will have an error between 10-20%. As the optical depth of the transmissometer path increases, the error in measured extinction drops rapidly to something less than 5%.

Integrating Nephelometer

The integrating nephelometer differs conceptually from the methods discussed above, in that it measures the light scattered from the aerosol, whereas the other methods measure a change in radiance or transmittance due to scattering and absorption. The geometry of the instrument is such (see, for example, the description in reference 7) that the signal is proportional to the scattering portion of b_{ext} , namely b_{scat} . This is an advantage in clean environments, because a small quantity is measured directly rather than being derived from a difference or ratio of larger numbers and, in fact, commercially-available integrating nephelometers can reliably measure b_{scat} due to Rayleigh scattering from gases. On the other hand, the optical signal is so small that it has been measured most successfully in a totally dark, closed chamber, free of stray light.

The closed chamber and instrument geometry result in several considerations concerning the use of the instrument for determining atmospheric extinction:

- o The measurements are totally independent of meteorological conditions and illumination, and they directly measure one component of extinction free of extraneous effects.
- o The sample must be drawn through ducts into a chamber which, in practice, is a different environment from the ambient. This can result in modification of the aerosol due to impaction on surfaces and because of heating or cooling. Although careful design can minimize these effects, they are difficult to avoid totally.
- o The need for sampling means that the atmospheric sample is representative of the measurement point, rather than of a larger area. Care has to be taken to assure that such samples are representative.
- o The instrument is unable to measure light scattering in the extreme forward and backward directions, typically within 8-10° of the axis. For particles larger than a few micrometers in diameter, a substantial fraction of the scattering is into the forward cone which is missed by the nephelometer, which means that the instrument underestimates the scattering from larger particles.

In addition to the above, the nephelometer only measures scattering, and not the portion of extinction due to absorption.

The errors caused by the various factors noted above vary from location to location. Heating of sample by the instrument, by even a few degrees Celsius, can cause errors approaching 100% at high humidities when the particles deliquesce.^{11,12} Forward angle truncation typically results in about 10% underestimates^{13,14} (after allowing for the fact that calibration of the instrument with a Rayleigh scattering gas compensates for some of the truncation error). The inability to measure absorption accounts for another 10% or so. Thus, the nephelometer systematically underestimates b_{ext} by roughly 20% in a "typical" dry aerosol atmosphere and by larger amounts under other conditions.

Results

Artificial Target Measurements

Figure 3 shows a plot of the October 9, 1985 "raw" teleradiometer readings associated with the artificial black target. The highest readings correspond to sky radiance, while the lower readings are proportional to the path radiance between the observation point and black target. The "relative radiance" reading for the path radiance can be arrived at by dividing the y-axis scale in Figure 3 by a factor of 2. From the hours 00 to 6:00 a.m. and 6:00 p.m. to 12 midnight, the sun is down and the teleradiometer reads zero radiance. The effects of clouds on lighting conditions are reflected in teleradiometer readings between 6:00 a.m. and 12:00 noon. From 12:00 noon to 2:00 p.m. there were intermittent showers with enough rain during 12:00 noon to 1:00 p.m. to make teleradiometer readings drop to near zero at certain times. These readings were eliminated from the data set. Afternoon readings correspond to nearly cloud-free conditions. Notice how the sky and path radiance varies smoothly in time. The increase in path radiance at 4:00 p.m. (1600 hours) corresponds to an increase in particulate which was also measured by the transmissometer and nephelometer (see Figures 4 and 6).

The teleradiometer relative radiance readings were converted to atmospheric extinction through the use of equation 2 after correcting for flare. As discussed in previous sections, the artificial target teleradiometer has a

flare of very nearly 1% of the background sky radiance. Therefore, the path radiance readings were corrected for flare using:

$$tN_{3.3km} = tN'_{3.3km} - 0.01_sN_{3.3km} \quad 9)$$

where $tN'_{3.3km}$ is the measured path radiance, $_sN_{3.3km}$ is the measured sky radiance at the observation point, and $tN_{3.3km}$ is the corrected path radiance used to calculate the extinction coefficient. The subscript 3.3 km indicates that the artificial target was 3.3 km from the observation point.

Results of this calculation are shown in a time series plot for October 9, 1985 in Figure 6.

Transmissometer Measurements

Raw transmissometer readings are shown for October 1985 in Figure 4. The data points are the result of one minute averages of the irradiance difference between the light being "on" and "off". The rain episodes discussed in previous sections are indicated in the figure as well as typical "high frequency" and "low frequency" turbulence conditions. Atmospheric turbulence is used to refer to a phenomenon of photon refraction by adjacent parcels of air that are at different temperatures and densities. These air parcels act as atmospheric lenses causing the photons to deviate from a straight line path. The net effect of these air parcels is to cause the light source to appear as if it were twinkling, much as a star appears to twinkle, or city lights appear to twinkle when viewed from a mountain top. Depending on parcel size and speed the air parcels move through the sight path, the apparent twinkle can be high frequency or low frequency in nature, taking as long as 10 or 15 minutes to cross the sight path. If the distribution of these air parcels are random, then as much light is bent out of the sight path as into it and the effect can be averaged out by simply averaging the signal over an appropriate time interval. If, however, light is preferentially bent out of the sight path, there is no way to process the received signal into meaningful physical variables.

Two objectives of this intercomparison were to determine how long the transmissometer signal, as represented in Figure 4, needed to be averaged to obtain a stable signal and whether averaging of transmissometer signal resulted in irradiance measurements that could be used to make meaningful extinction coefficient measurements.

The first objective was examined by calculating the 90% confidence interval as a function of averaging time. These results are shown in Figure 5 for low and high frequency turbulence conditions. For a 3 minute averaging time, the confidence interval for high and low frequency conditions are ± 12 and ± 38 around a signal of approximately 150. After a 30 minute averaging time, the high and low frequency confidence intervals asymptotically approach ± 1 and ± 2.5 . An averaging time much beyond 30 minutes will not yield significant increases in confidence of measured signal.

Figure 6 shows the results of transmissometer extinction calculations for October 9, 1985. Also presented in Figure 6 are extinction and scattering derived from natural and artificial target contrast teleradiometer and nephelometer measurements. Table 2 and Figures 7 through 9 summarize intercomparison between each of the methods used for calculating extinction. In Table 2, measurements are compared to each other and since teleradiometer measurements were made only during daylight hours, daytime transmissometer and nephelometer extinctions were also computed. Various statistical descriptions

were calculated. The absolute difference (AD) and average bias (AB) were calculated using

$$AD = \sum \frac{2}{N} \left| \frac{E_1 - E_2}{E_1 + E_2} \right| \quad 10)$$

$$AB = \sum \frac{2}{N} \left| \frac{E_1 - E_2}{E_1 + E_2} \right| \quad 11)$$

where N is number of data points and E_1 and E_2 are elements in the data set. Also listed are the correlations between each of the variables. Slopes of the regression line comparing two measurements were carried out using "perpendicular" departure rather than conventional regression analysis since there is error in both dependent and independent variables. The details of the regression model used in this paper are presented in Appendix A.

The highest correlations of approximately 0.80 were between daytime transmissometer (Tran), artificial black target (BT) and daytime nephelometer (Neph) extinctions. However, nephelometer measured scattering coefficients are about 40% lower than either black target or transmissometer derived extinction. Scatter plots of the BT versus Tran and daytime Neph versus daytime Tran are shown in Figures 7 and 8. If the instruments were to measure true extinction the slope of the regression line between extinction derived from various measurement techniques would equal one. The slope of the regression line between BT and transmissometer extinction of 1.07 ± 0.07 is not significantly different from one. While the slope between nephelometer and BT or Tran extinction is 0.53 ± 0.05 . Not surprising, comparison of natural target teleradiometer extinction to Tran or BT extinction is, within statistical error, near one, 0.90 ± 0.133 and 0.90 ± 0.091 respectively. However, because of meteorological effects, teleradiometer derived extinction using natural targets when compared to other measurement techniques result in larger standard errors and correlations that are lower. Figure 9 graphically shows the scatter between natural target teleradiometer derived extinction and extinction obtained from transmissometer measurements. Comparison of transmissometer extinction with nephelometer scattering for both daytime and nighttime measurements shows a significant reduction in correlation. It is hypothesized that during stable nighttime conditions "pockets" of air carrying wood fire smoke from nearby sawmills drifted into the measurement area. Examination of time plots show large excursions in extinction at both nephelometer and transmissometer sites. However, nephelometer readings were always lower by at least a factor of two.

Conclusions

Two methods most commonly used for estimating atmospheric extinction are teleradiometric contrast measurements of natural targets and integrating nephelometer measurements of the atmospheric scattering coefficient. Both techniques have serious shortcomings. The nephelometer has an enclosed sampling chamber and as such does not measure scattering from large particles that do not pass through the instrument, it may inadvertently modify aerosols, and it does not measure the effects that absorbing aerosols have on overall extinction. On the other hand, extinction derived from teleradiometer measurements of contrast of a single natural target properly reflects the influences of large as well as small particles, and measures the effects of scattering and absorption. However, the contrast measurement is also sensitive to meteorological factors that do not have anything to do with

atmospheric extinction, such as shading of sight path and bright or dark clouds behind the target which alter inherent contrast.

Radiation transfer calculations suggest that a short path artificial black target, $C_0 = -0.1$, teleradiometric measurement should yield quite accurate extinction approximations. Clouds behind the target and at distances beyond 100 km do not affect the calculation to a large degree nor do clouds over the sight path as long as the sight path to the target is illuminated the same way as the sight path over the target looking at the background sky.

The transmissometer, like the nephelometer, is not affected by meteorological or lighting conditions. However, it is not clear apriori that varying atmospheric turbulence conditions do not effect the amount of light arriving at the receiver and as such yield spurious irradiance measurements which are independent of atmospheric aerosol loading.

Since a "standard" method for making extinction measurements does not exist nor is there a "standard atmosphere" that can be introduced into the various instrument configurations, it is not possible to compare the measurements to the "right" answer and evaluate instrument sensitivity and accuracy. Rather, what must be looked for is consistency between various measurement of extinction and comparison to these measurements to what might be expected from theoretical radiation transfer calculations.

It can be argued that the black artificial target contrast measurement, being the simplest and most straightforward measurement, should yield a good approximation of atmospheric extinction. Extinction derived from transmissometer measurements compare quite favorably to black target contrast measurements. The correlation between the two measurements is 0.80 and slope of a perpendicular departure regression line comparing the two measurements of extinction does not statistically differ from one. On the other hand the integrating nephelometer measurements are on average over 40% lower than either black target or transmissometer extinction. As expected, the slope between natural target extinction and the transmissometer or black target extinction is near one, but the correlation is reduced because of scatter introduced into natural target extinction by variations in meteorological conditions.

Appendix A

For intercomparison of data derived from two measurement methods, the usual least squares regression is often not appropriate. This is due to the fact that data obtained from both measurement methods are contaminated with measurement errors. The more appropriate approach is to use the so called 'errors in variables regression model'. There is a vast amount of literature on this subject, but an adequate background for applications can be obtained from a paper by Mandel.¹⁵ (1984, Journal of Quality Technology).

Let (X_i, Y_i) $i=1,2,\dots,n$ denote the data obtained from two measurement methods where X_i denote readings from instrument A and Y_i from instrument B. Suppose that the true values being measured are denoted by w_i . If both instruments have a zero shift and a bias, then:

$$\text{and } X_i = \alpha_1 + \beta_1 w_i + v_i \quad A1)$$

$$Y_i = \alpha_2 + \beta_2 w_i + \epsilon_i \quad A2)$$

where v_i, ϵ_i denote random errors. Eliminating w_i between the above two equations, the relationship between Y_i and X can be written in the form

$$\text{where } y_i = \alpha + \beta x_i \quad A3)$$

where

$$Y_i = y_i + \epsilon_i \quad A4)$$

and

$$X_i = x_i + v_i . \quad A5)$$

Here y_i and x_i denote the readings from instrument A and instrument B respectively in the absence of random errors. The coefficients α and β stand for the relative zero shift and the relative bias respectively. If the two instruments agree on the average, then α should be zero and β should be 1.

Suppose that the random error ϵ_i associated with the Y_i has mean zero and variance σ_ϵ^2 and the random error v_i associated with X_i has mean zero and variance σ_v^2 . Let the ratio $\sigma_\epsilon^2/\sigma_v^2$ be represented by λ . We assume that this ratio can be experimentally determined and hence, for all practical purposes, known. The formulas for calculating estimates a and b of α and β respectively along with their standard errors are shown below. The formulas for the standard errors are approximate and exact formulas are not available.

$$\left. \begin{aligned} b &= \frac{(SY Y - \lambda SX X) + \{(SY Y - \lambda SX X)^2 + 4 \lambda SX Y^2\}^{1/2}}{2 SX Y} \\ a &= \bar{Y} - \beta \bar{X} \end{aligned} \right\} \quad A6)$$

where

$$\begin{aligned}SYY &= \sum (Y_i - \bar{Y})^2 \\SXX &= \sum (X_i - \bar{X})^2 \\SXY &= \sum (X_i - \bar{X})(Y_i - \bar{Y})\end{aligned}\tag{A7}$$

and
 \bar{X} = the mean of X_1, \dots, X_n
 \bar{Y} = the mean of Y_1, \dots, Y_n .

To compute the standard errors of these coefficients, it is convenient to first calculate the following intermediate quantities.

$$\begin{aligned}SUU &= SXX + 2 b SXY + b^2 SYY \\SVV &= SYY - 2 b SXY + b^2 SXX\end{aligned}\tag{A8}$$

and

$$s_e = [SVV / (n-2)]^{1/2} .\tag{A9}$$

We then have

$$s.e.(a) = s_e \left[\frac{1}{n} + \frac{\bar{X}^2(1+b^2)^2}{SUU} \right]^{1/2}\tag{A10}$$

and

$$s.e.(b) = s_e \left[(1+b^2)^2 / SUU \right]^{1/2} .\tag{A11}$$

Approximate 95% confidence intervals on α and β can be obtained in the usual manner by computing the limits as estimate plus two standard errors and estimate minus two standard errors.

For calculations in this paper it was assumed that $\lambda = 1$ (that is, the measurement error variances for the different measuring methods are roughly equal). The calculation of a and b then reduces to computing the estimates of a and b by minimizing the sum of squares of the perpendicular distances from the data points to the fitted line. We can also compute a figure of merit for the degree of agreement between the two instruments. For the case $\lambda = 1$, this can be done as follows: Calculate the sum of squares of the perpendicular distances from the data points to the line of best fit defined in (A6). Let this quantity be denoted by SPD1. Also calculate the sum of squares of the perpendicular distances from the data points to the line $Y = X$. Let this be denoted by SPD2. Let R denote the ratio SPD1 / SPD2. The value of R is always between 0 and 1. If the line of best fit is not too different from the line $Y = X$ (which corresponds to perfect agreement between the two instruments apart from random errors) then the ratio R should be very close to 1.

The assumptions, findings, conclusions, judgments and views presented herein are those of the authors and should not be interpreted as necessarily representing official National Park Service policies.

References

1. Charlson, R.J., H. Horvath, and R.F. Pueschel, "The Direct Measurement of Atmospheric Light Scattering Coefficient for Studies of Visibility and Pollution," Atmos. Environ. 1: 469 (1967).
2. Malm, W.C., and J.V. Molenar, "Visibility Measurements in National Parks in the Western United States," APCA Journal 34 (9): (1984).
3. Malm, W.C., "Review of Techniques for Measuring Atmospheric Extinction," Paper 86-17.2, presented at the 79th Annual Meeting and Exhibition of the Air Pollution Control Association, June 22-27, 1986, Minneapolis, Minnesota.
4. Instrument specifications available from Aerovironment, Inc., 825 Myrtle Avenue, Monrovia, CA 91016-3424.
5. Instrument specifications available from OPTEC, Inc., 199 Smith Road, Lowell, MI 49331.
6. Aerovironment, Inc., 825 Myrtle Avenue, Monrovia, CA 91016-3424.
7. Malm, W.C., "Considerations in the Measurement of Visibility," APCA Journal 29: 1042 (1979).
8. Middleton, W.E.K., Vision Through the Atmosphere, University of Toronto Press, Toronto, Ontario, Canada, 1958.
9. Davis, J.M., T.B. McKee, and S.K. Cox, "An Investigation of the Application of the Monte Carlo Method to Problems in Visibility Using a Local Estimate," presented at the International Association of Meteorology and Atmospheric Physics' International Radiation Symposium, Perugia, Italy, August 21-29, 1984.
10. Hall, J.S. and L.A. Riley, Proceedings of AIAA 10th Thermophysics Conference, 75: 683 (May 1975)
11. Dzubay, T.G. R.K. Steven, C.W. Lewis, D. Hern, W.J. Courtney, J.W. Tesch, and M.A. Mason, "Visibility and Aerosol Composition in Houston, Texas," Environ. Sci. and Tech., 16: 514 (1982).
12. Tombach, I. and D. Allard, "Comparison of Visibility Measurement Techniques: Eastern United States." Report EPRI EA-3292, Electric Power Research Institute, Palo Alto, CA (1983).
13. Ensor, D.S. and A.P. Waggoner, "Angular Truncation Error in the Integrating Nephelometer," Atmos. Environ., 4: 481 (1970).
14. Quenzel, H., G.H. Ruppertsberg and R. Schellhase, "Calculations About the Systematic Error of Visibility-Meters Measuring Scattered Light," Atmos. Environ., 9: 587 (1975).
15. J. Mandel, "Fitting straight lines when both variables are subject to error," Journal of Quality Technology, 16: 1 (1984).

Table 1. Description of physical layout of teleradiometers used in the intercomparison experiment.

INSTRUMENT	ANGLE OF VIEW	FOCAL LENGTH	TARGET DISTANCE	AZIMUTH ANGLE	OBSERVATION ANGLE	TARGET CHARACTERISTICS	FILTER CHARACTERISTICS
Teleradiometer (natural target)	0.034°	500 mm	63.0 km	303.5°	Not Available	Large Forested Mountain	550 nm ± 10 nm
Teleradiometer (artificial target)	0.017°	762 mm	3.3 km	325.0°	+0.1°	Artificial Black Target	550 nm ± 10 nm
Teleradiometer (transmissometer)	0.07°	630 mm	7.8 km	0.0°	-1.54°	Artificial Light Source	550 nm ± 10 nm

Table 2. Statistical tests for 60 minute averaged data.

	<u>BT^a/Tran^b</u>	<u>Nat^c/Tran</u>	<u>Neph^d/Tran</u>	<u>Neph(D)/Tran(D)*</u>	<u>Nat/BT</u>	<u>Neph/BT</u>	<u>Neph/Nat</u>
Slope	1.07 ± 0.074**	0.90 ± 0.133	0.48 ± 0.038	0.53 ± 0.055	0.90 ± 0.091	0.53 ± 0.055	0.58 ± 0.11
Intercept	-0.003 ± 0.003	0.002 ± 0.004	0.003 ± 0.001	0.003 ± 0.002	0.003 ± 0.002	0.003 ± 0.002	0.002 ± 0.003
Correlation	0.80	0.49	0.68	0.79	0.70	0.75	0.42
R Square	63.76	23.96	46.92	63.24	48.15	56.52	17.36
F-Value	75.66	10.71	97.24	87.75	34.36	57.20	8.40
Absolute Difference	0.15	0.19	0.54	0.43	0.12	0.42	0.40
Average Bias	0.03	0.02	0.54	0.43	0.02	0.42	0.37

* daytime readings
 ** standard error
 a Black Target
 b Transmissometer
 c Natural Teleradiometer Target
 d Nephelometer

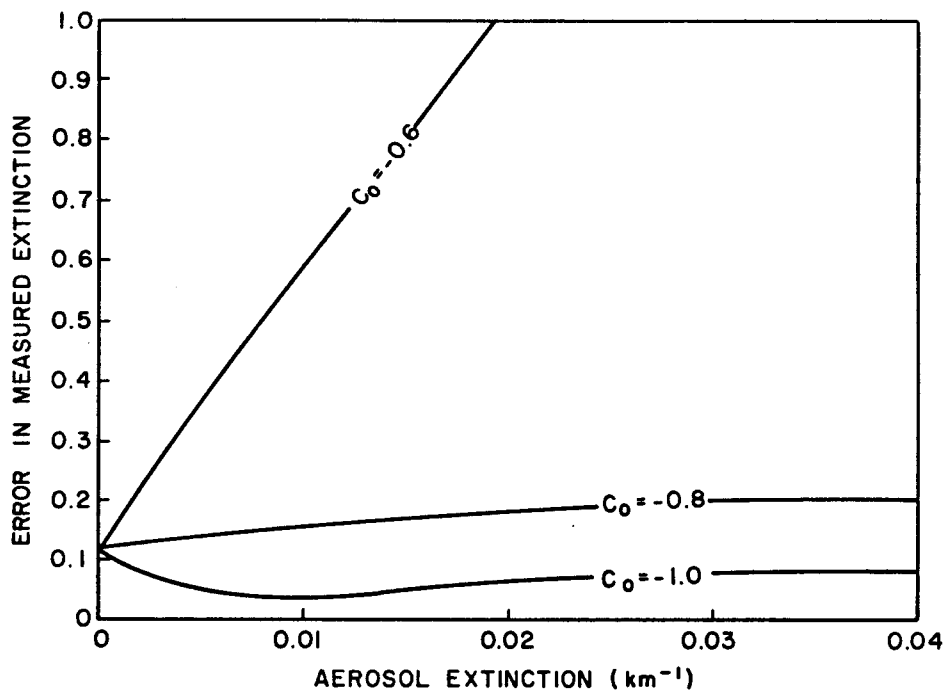


Figure 1. Error in teleradiometer derived atmospheric extinction as a function of atmospheric extinction for three typical values of inherent contrast.

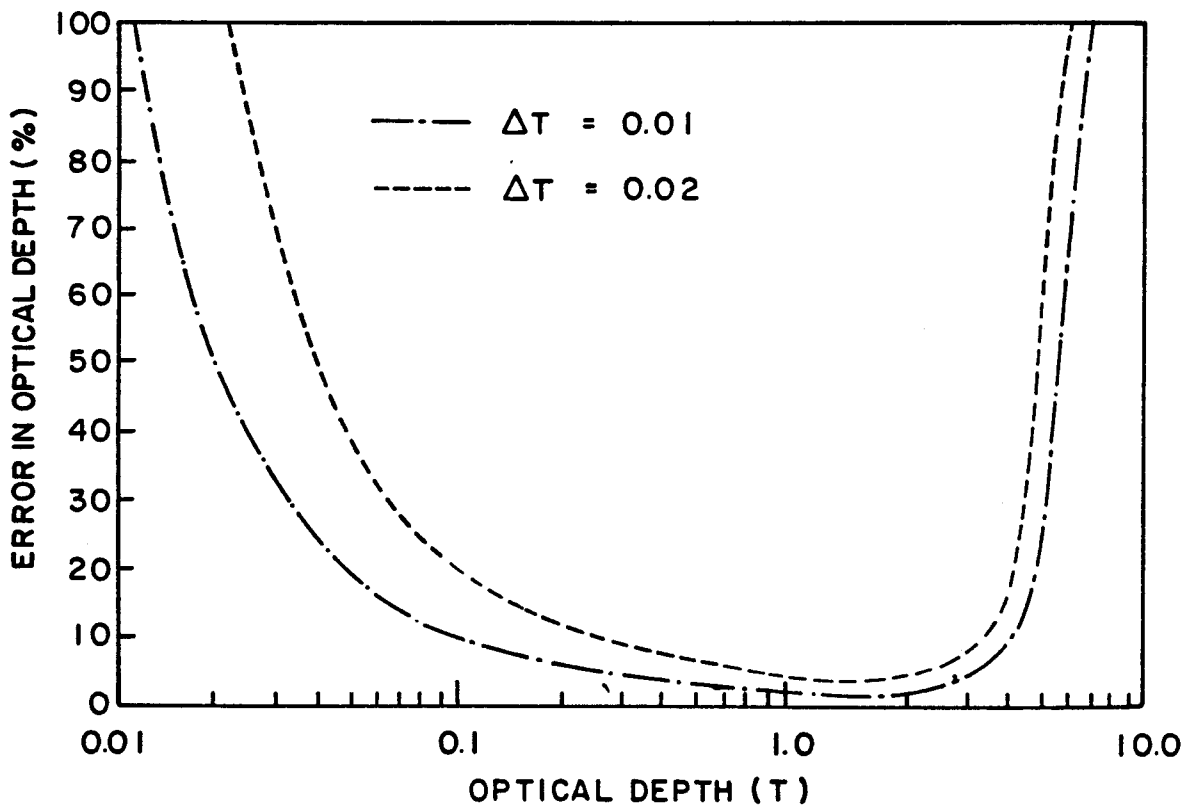


Figure 2. Error in transmissometer measured optical depth as a function of optical depth for $\Delta T = 0.01$ and 0.02 .

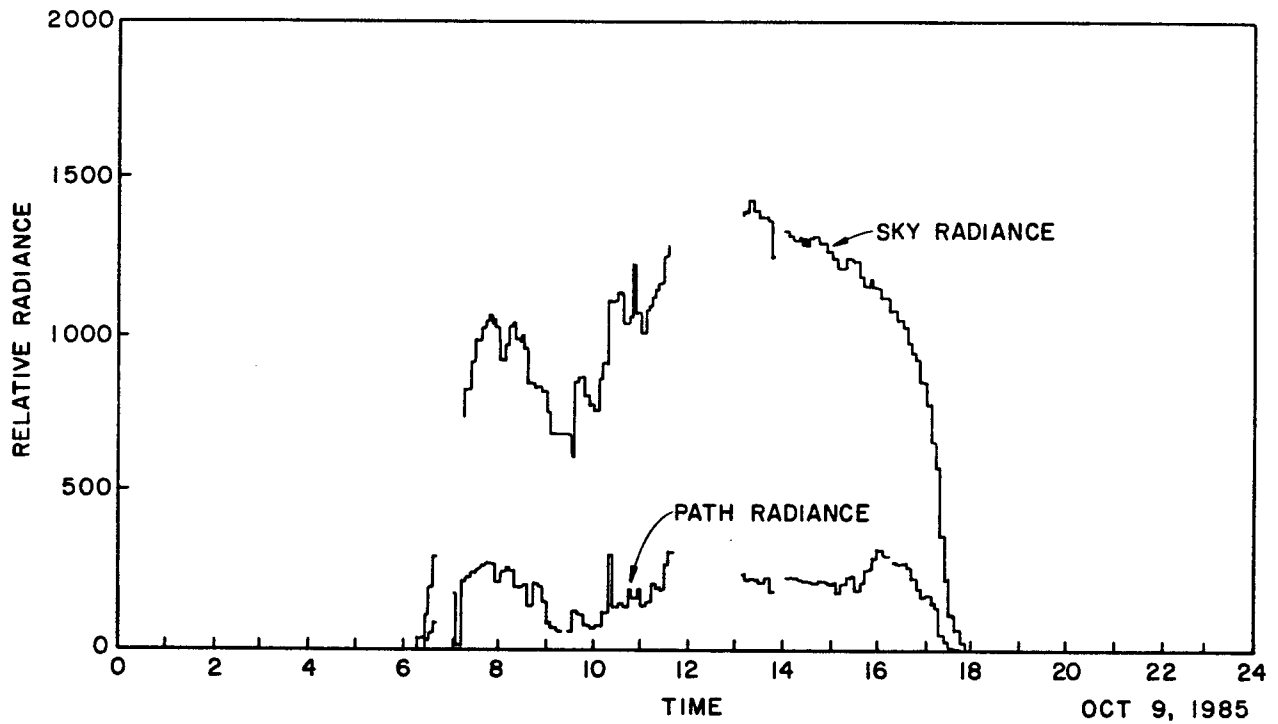


Figure 3. Relative artificial black target sky and path radiance plotted as a function of time for October 9, 1985. Relative path radiance is equal to the y-axis relative radiance values divided by two.

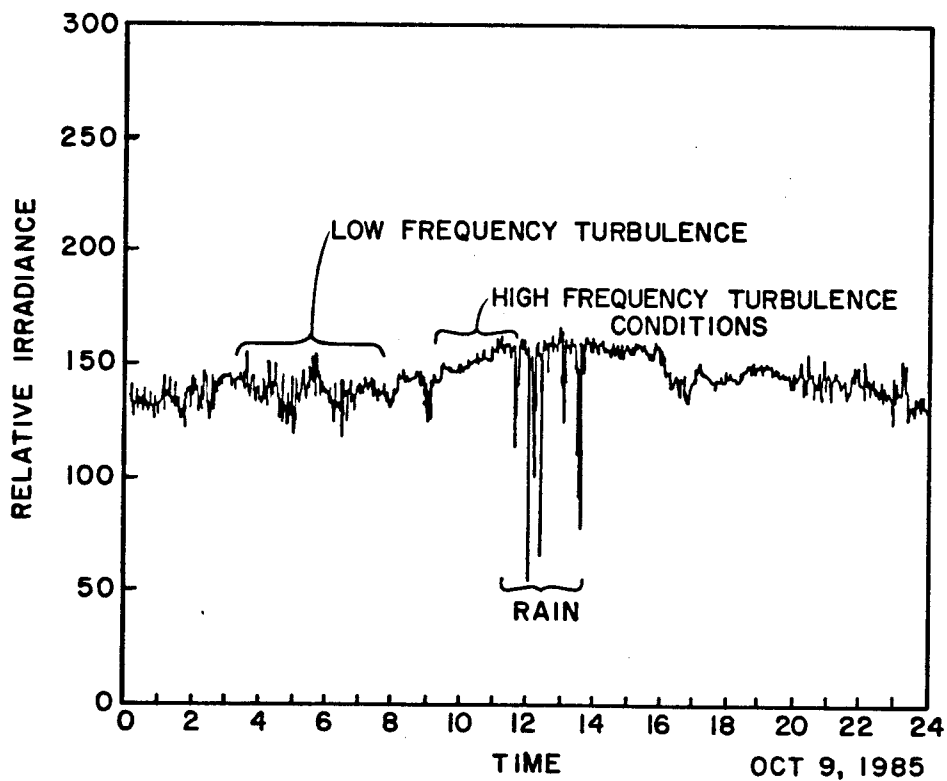


Figure 4. Transmissometer relative irradiance is plotted as a function of time for October 9, 1985. Examples of low and high frequency turbulence conditions are indicated on the graph.

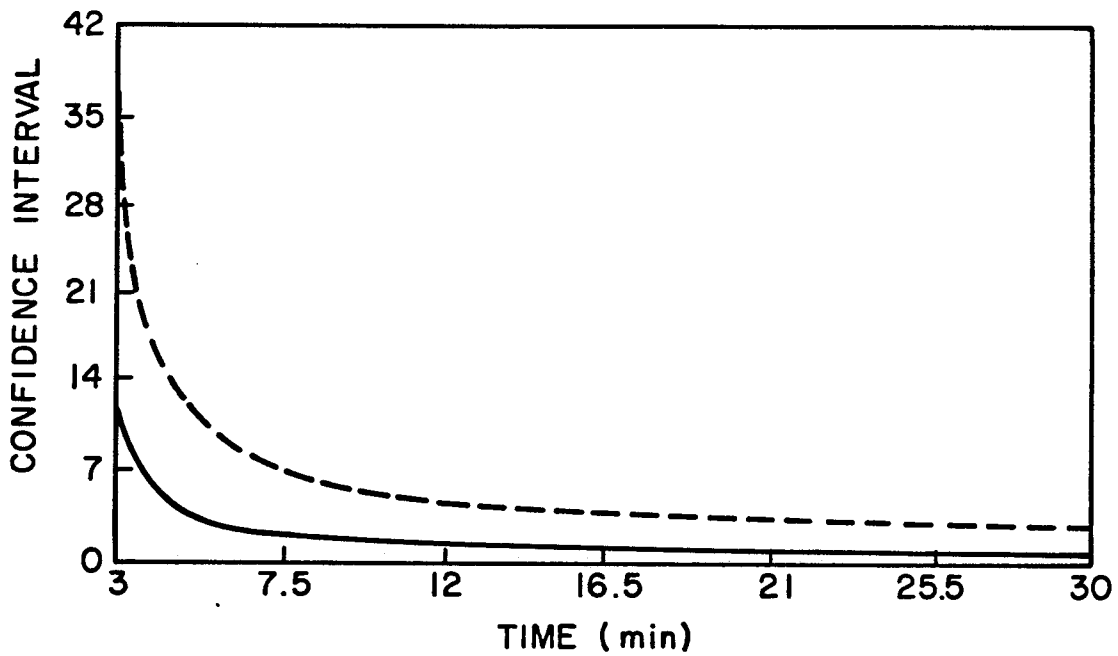


Figure 5. 90% confidence interval around average relative transmissometer receiver irradiance measurements are plotted as a function of signal averaging time. ---- corresponds to high turbulence conditions, while solid line represented low turbulent conditions.

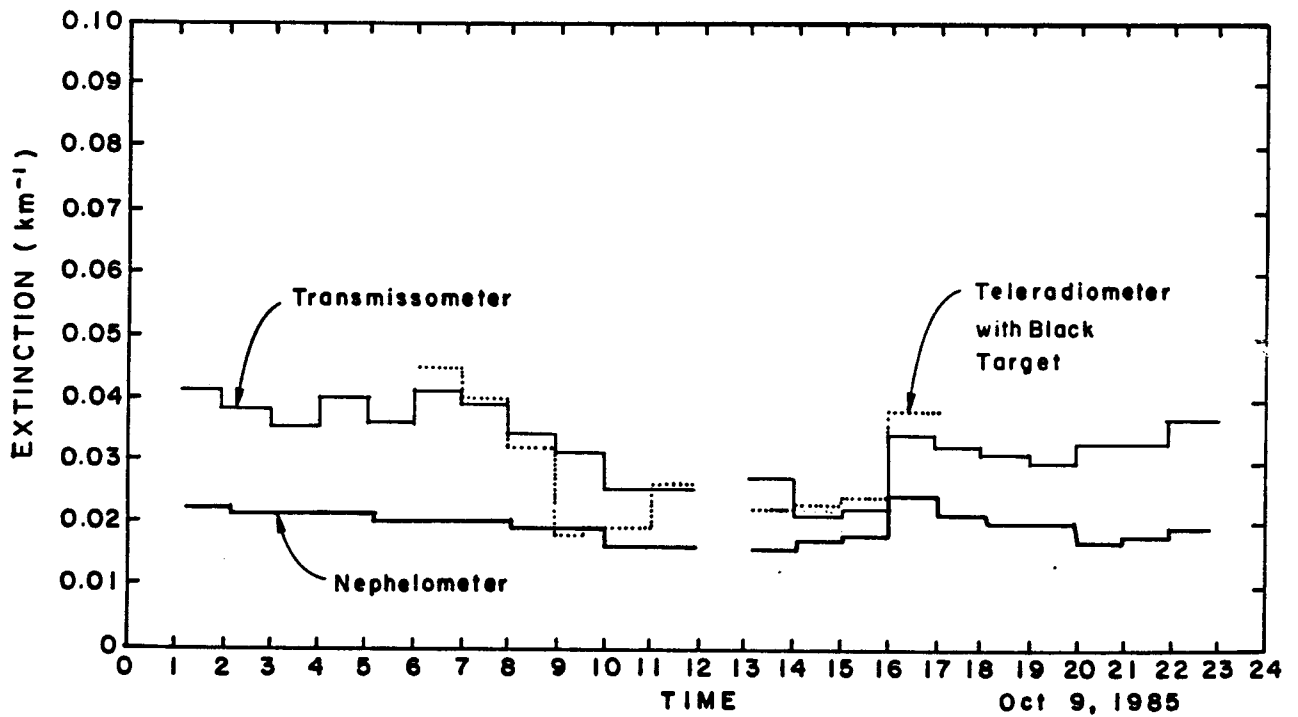


Figure 6. Atmospheric extinction derived from transmissometer, nephelometer and teleradiometer measurements of artificial black target contrast are plotted as a function of time on October 9, 1985. Extinctions for each measurement were averaged over one hour.

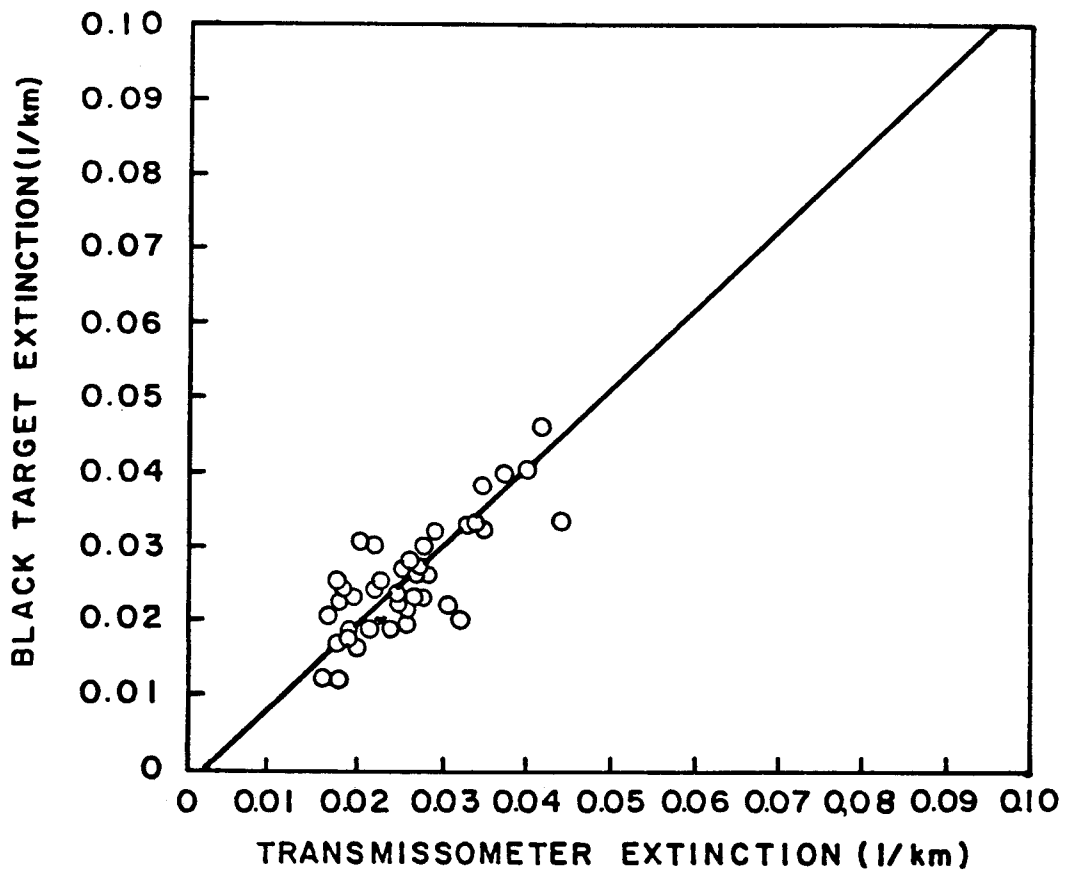


Figure 7. Scatterplot of black target and transmissometer atmospheric extinction. Slope of regression line equal to 1.07 ± 0.074 and intercept is equal to -0.003 ± 0.003 .

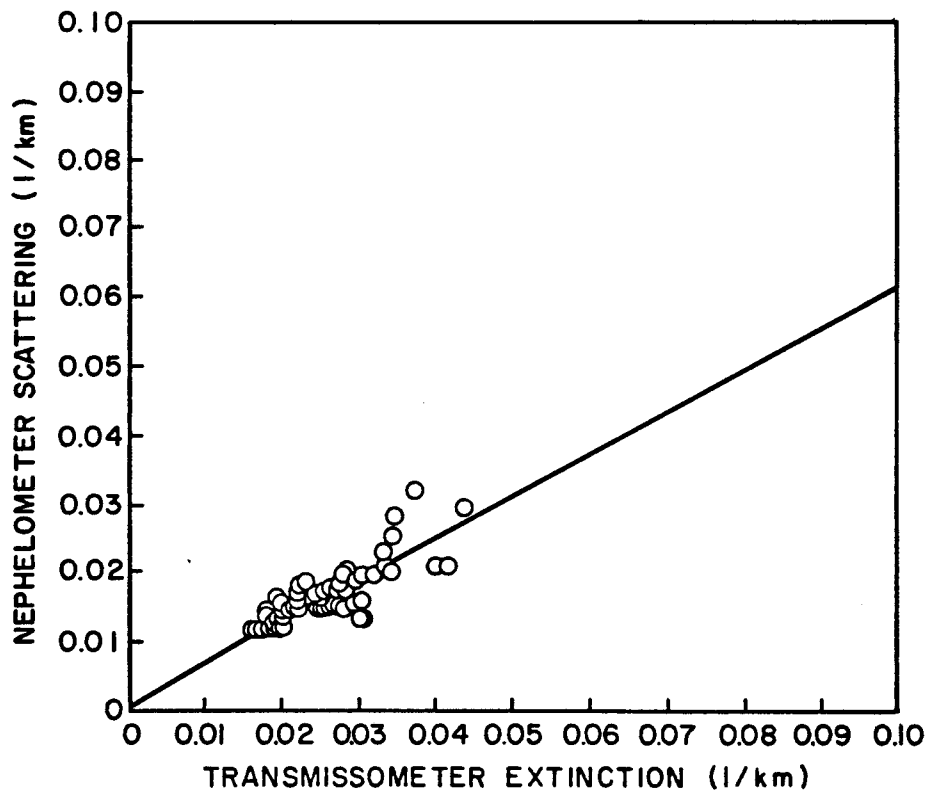


Figure 8. Scatterplot of "daytime" integrating nephelometer scattering and transmissometer extinction. Slope of regression line is 0.53 ± 0.055 and intercept is equal to 0.003 ± 0.002 .